

SEISMO-TECTONIC DEFORMATIONS OF THE EARTH'S CRUST OF THE ANATOLIA PLATE (Türkiye)

N.A. Sycheva

Institute of Physics of the Earth. O.Yu. Schmidt RAS

The work was carried out within the framework of the state task of the IPE RAS

Study area

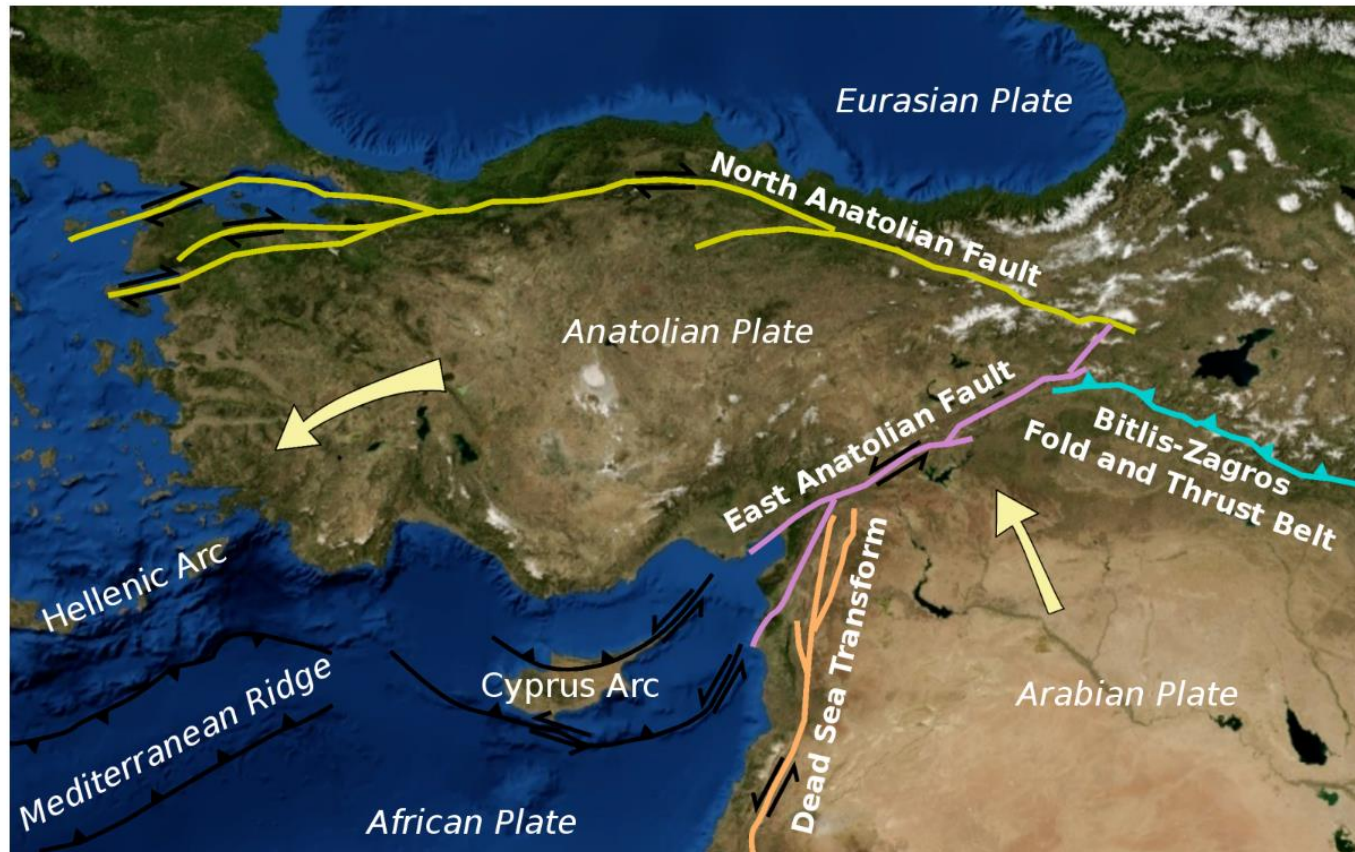


Fig. 1. Tectonic map of Turkey.

Turkey is a country known for its unique geography that bridges continents and cultures. It also bridges several tectonic plates including the Eurasian, African, and Arabian plates through the Anatolian plate [Bommer et al., 2002]. Interactions between all surrounding plates and the Anatolian plate produce an active seismic region that encompasses most of Turkey.

Earthquake February 6, 2023

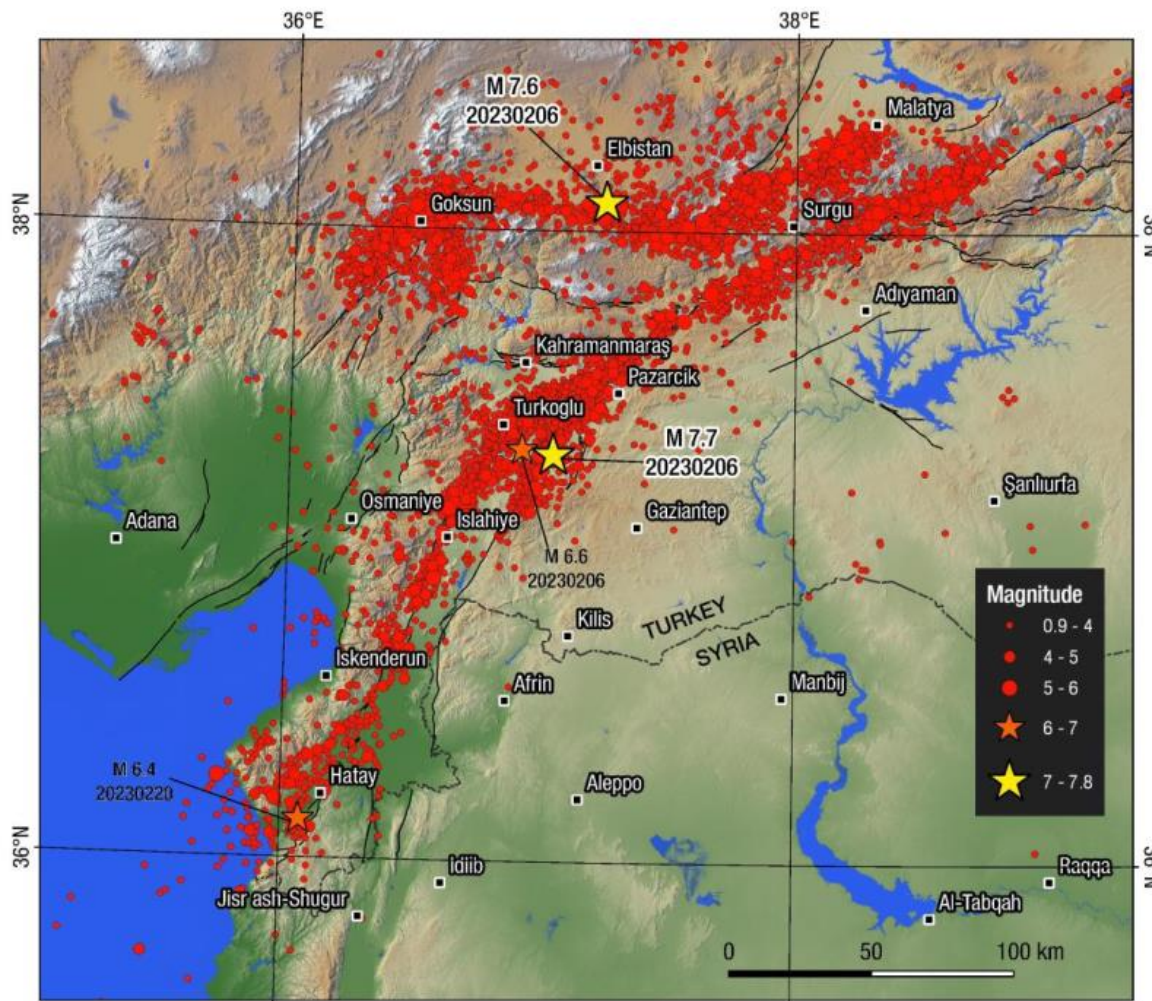


Fig. 2. Double strongest earthquake (**Mw 7.8 and Mw 7.6**) and its aftershocks [Taftoglou et al., 2023].

On **February 6th, 2023**, a devastating earthquake doublet (**Mw 7.8 and Mw 7.6**) shook south eastern Turkey and northern Syria, causing widespread damage, homelessness, and over fifty thousand fatalities [Dal Zilio and Ampuero, 2023]. The first quake (Mw 7.8) struck along the East Anatolian Fault (EAF), while the second (Mw 7.6) occurred on the Cardak Fault (CF), a splay fault linked to the EAF's Erkenek segment [Duman and Erme, 2013] (Fig. 2). Both shallow-depth main shocks (**10km-14.5km**) generated intense ground motion, leading to catastrophic regional impacts [Melgar et al., 2023; Okuwaki et al., 2023; Mai et al., 2023].

Earthquake February 6, 2023 [Zilio, Ampuero, 2023]

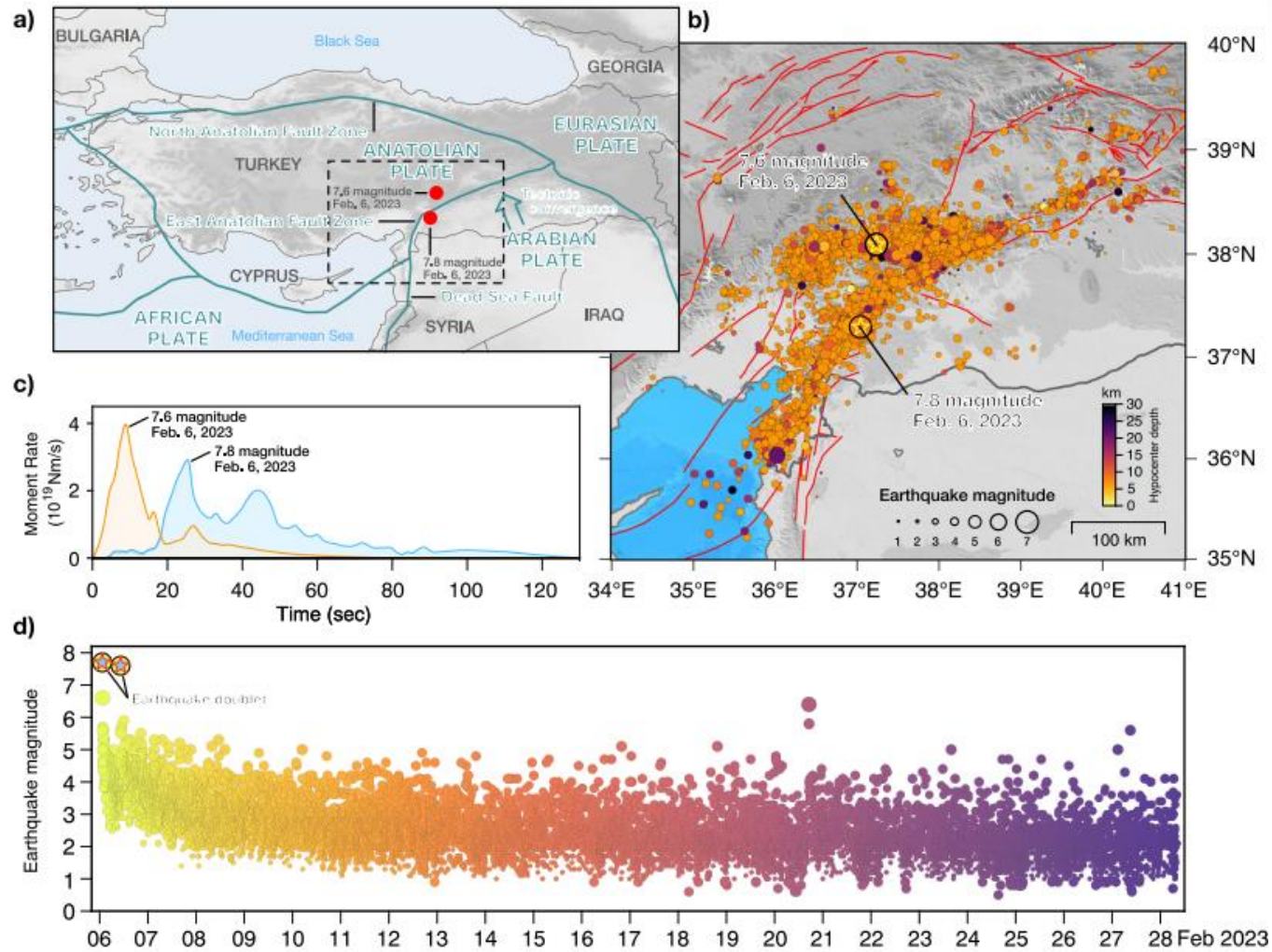


Fig. 3. Tectonic setting and seismicity caused by the 2023 Kahramanmaraş Earthquake Sequence. a The inset map shows the large-scale geodynamic context indicating the two main strike-slip faults that delineate the Anatolian block: the East Anatolian Fault and the North Anatolian Fault. Known and mapped surface traces of the main faults are shown as dark grey lines. b First month of relocated seismicity as a function of magnitude and depth, including the main two events and aftershocks. Fault lines are indicated in red. c Source time functions of both events of the main two events are provided by the US Geological Survey (USGS). d Temporal evolution of seismicity in the month of February 2023. The yellow-to-purple color scheme indicates the temporal evolution of seismicity. The two stars indicate the earthquake doublet. The seismic catalogue is provided by the Disaster and Emergency Management Authority of Turkey (AFAD).

Purpose

Seismicity analysis and evaluation of the stress-strain state based on the application of the seismotectonic deformation method (STD).

Pre-instrumental and instrumental strong earthquakes

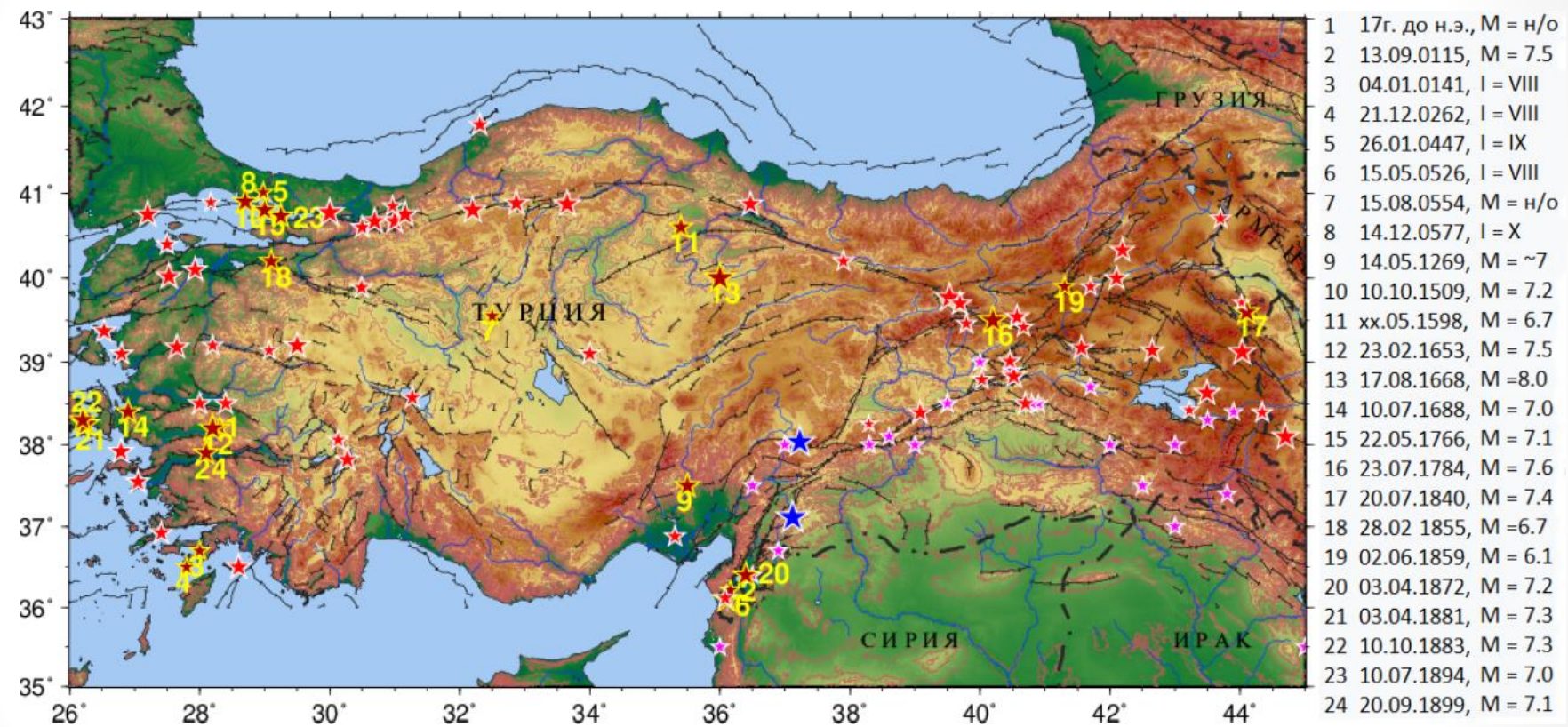


Fig. 4. Epicenters of strong earthquakes: dark red asterisks mark historical events that occurred before 1900 [List ...], red – strong earthquakes from 1900 to the present [List ...], pink – earthquakes from [Ambraseys, 1989] and blue – earthquakes that occurred on February 6, 2023 with MW = 7.8 and MW = 7.5 [Search Earthquake ...].

Seismicity and seismic stations

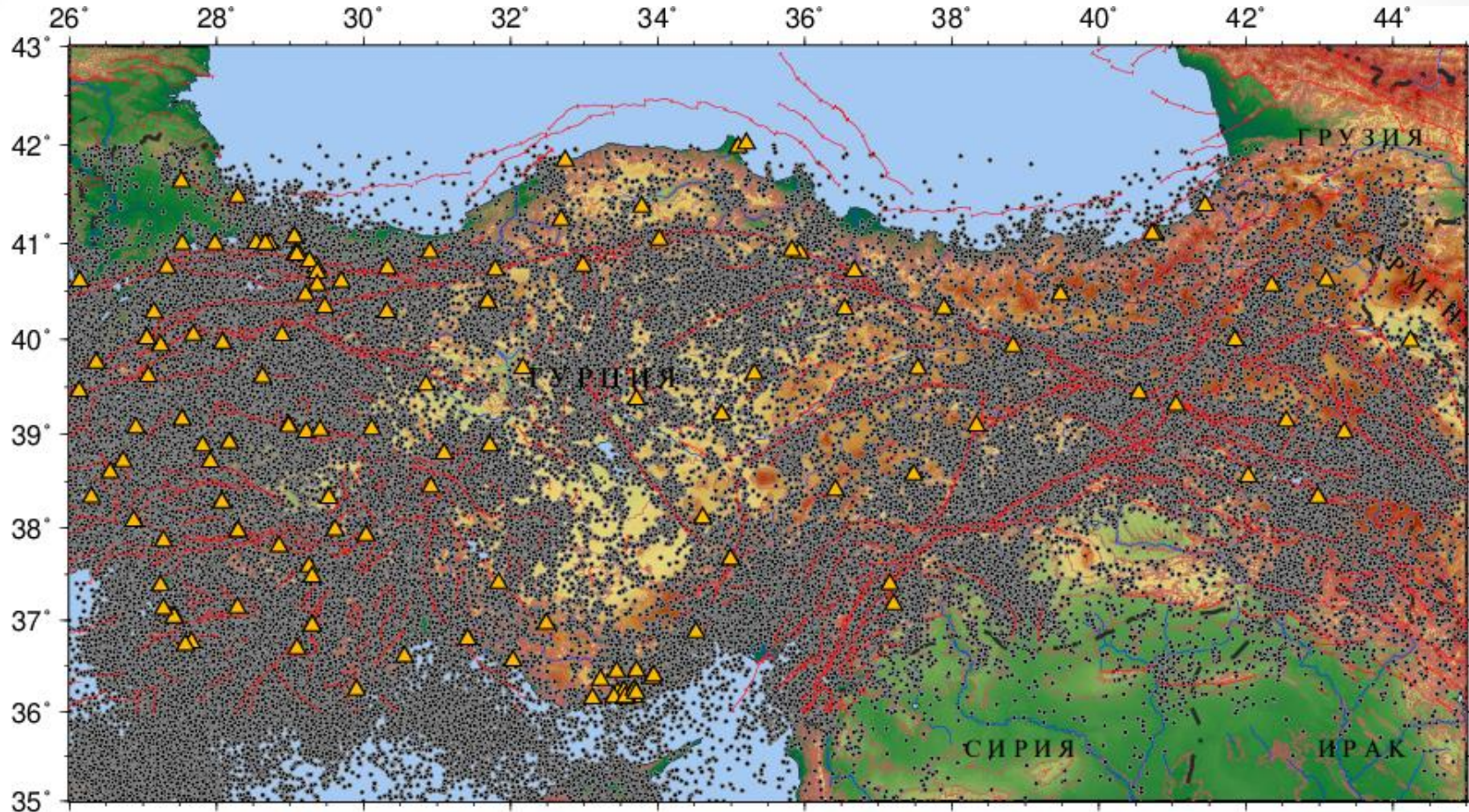


Fig. 5. Epicentral position of earthquakes (**332,201** events) that occurred from **1900 to 2022**. Triangles - seismic stations (**249**, for 2022) according to the Earthquake Research Institute ([BOUN KOERI](http://www.koeri.boun.edu.tr): <http://www.koeri.boun.edu.tr>).

Quantitative distribution of seismicity

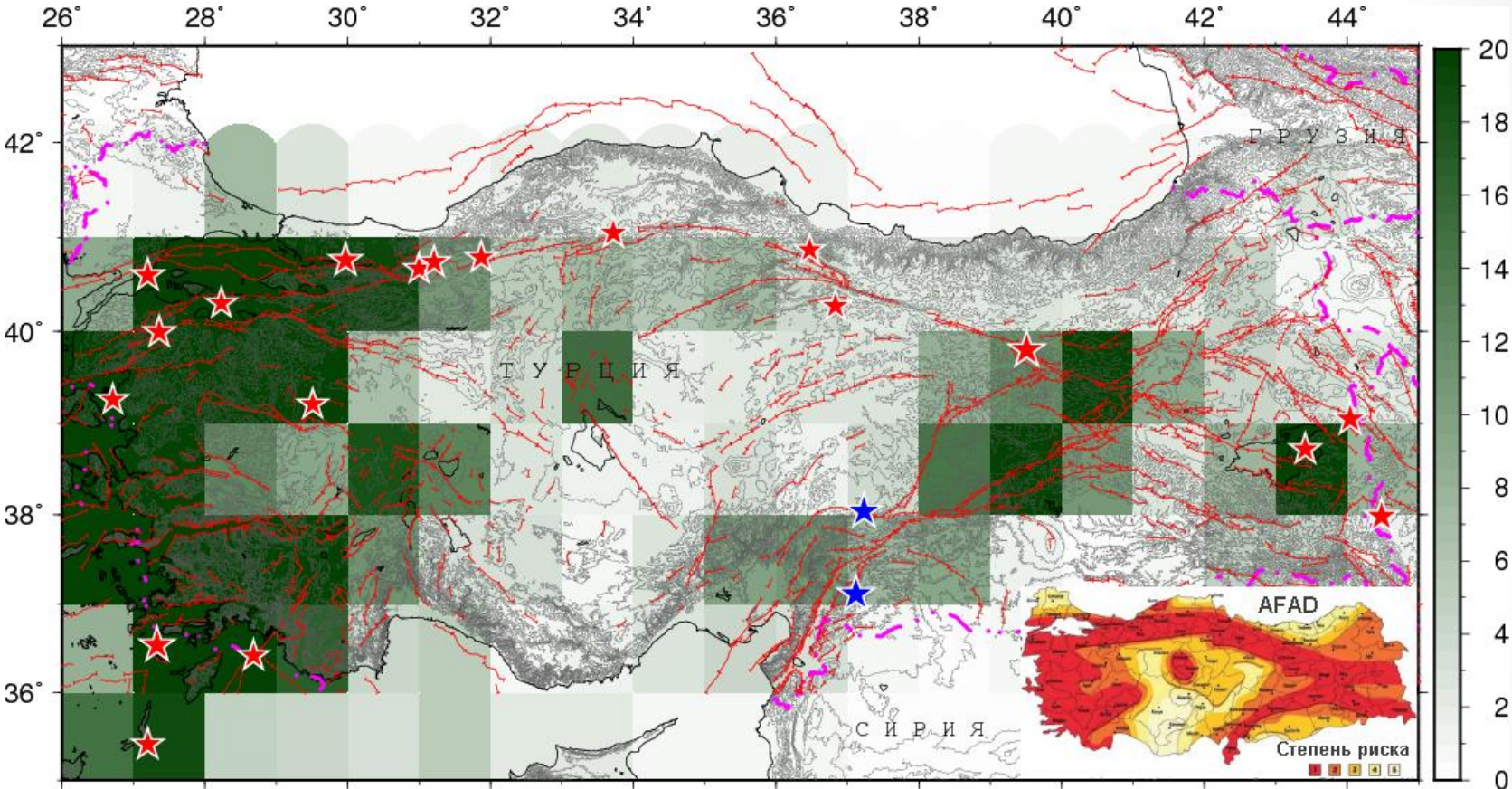


Fig. 6. Distribution of the number of earthquakes per year according to the earthquake catalog data. The inset shows the seismic risk map of Turkey [Gunes, 2015].

Input data. Focal mechanisms.

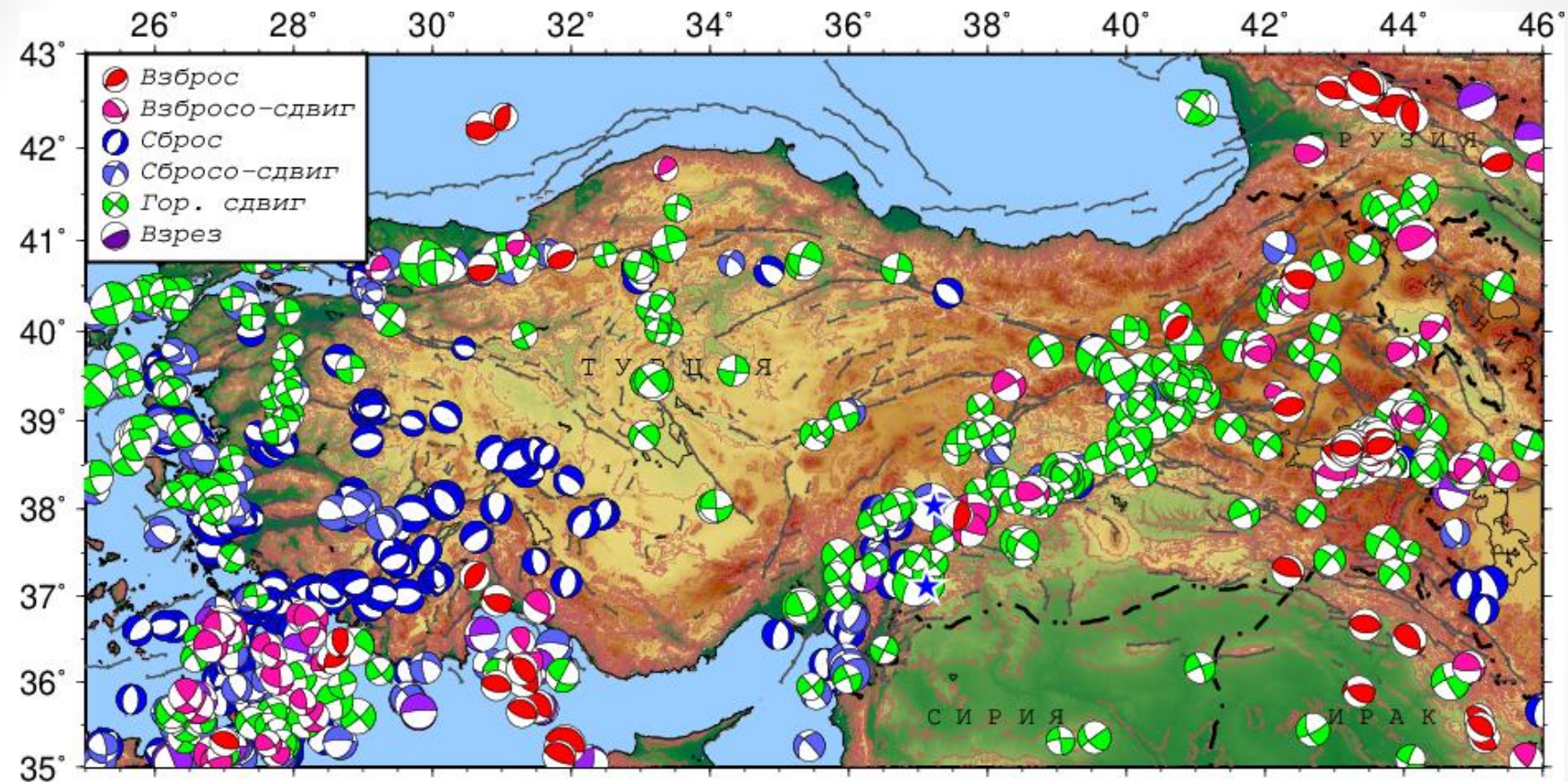


Fig. 7. Focal mechanisms of source (807 events, 1976-2023). The color of the mechanism indicates the type of movement according to the tab on the left. The blue asterisks are the epicenters of the earthquakes that occurred on 02.06.2023 with $M_w = 7.8$ and $M_w = 7.6$. The gray lines are local and regional faults according to [Bachmanov et al., 2017].

Quantitative characteristics of the FM catalog and the deep location of earthquakes

$4 \leq M \leq 5.5$

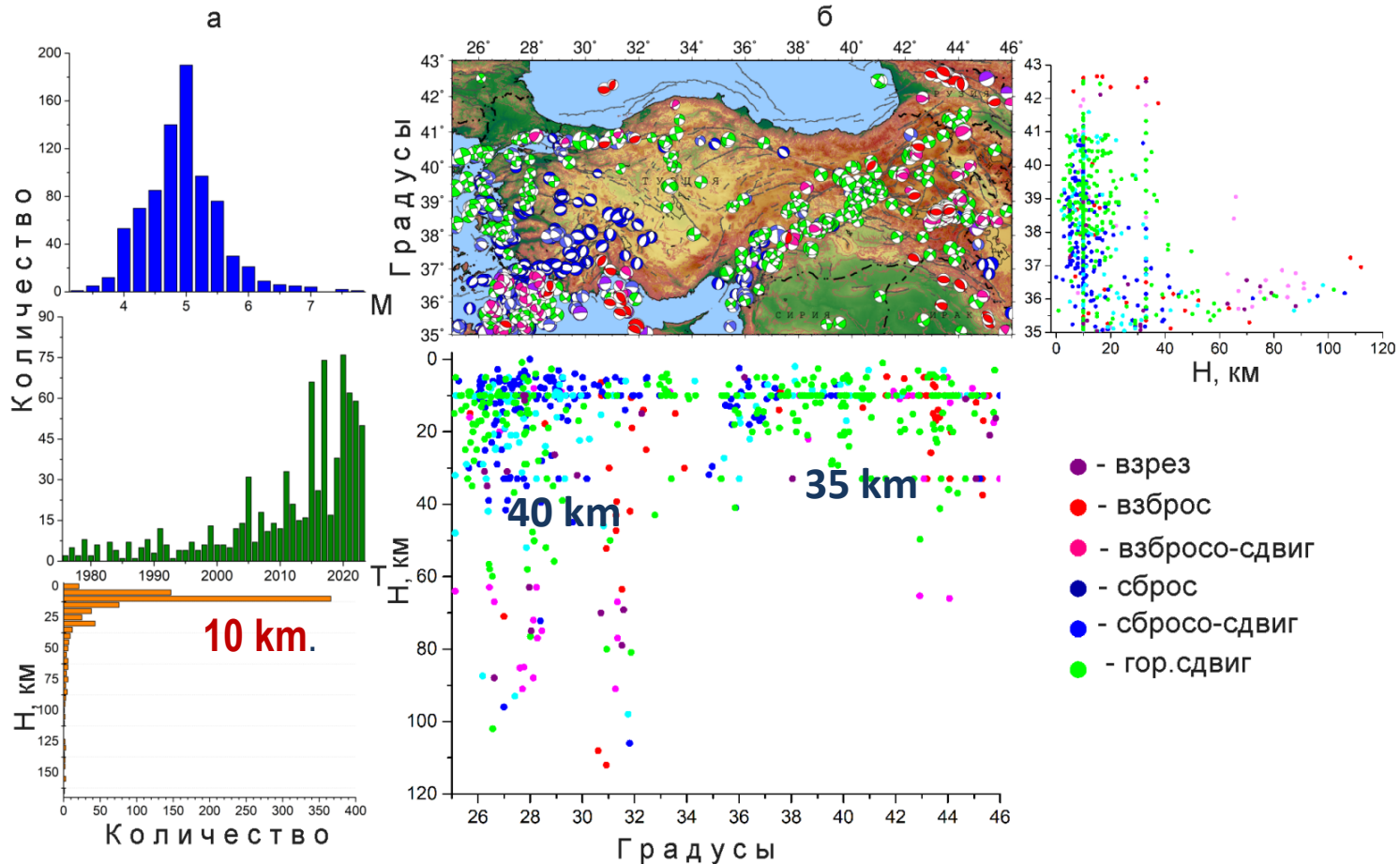


Fig. 8. Quantitative characteristics (a) and focal mechanisms (map) and vertical sections (b) of earthquake location: north-south; west-east .

Epicenters of earthquakes with $H > 50$ km

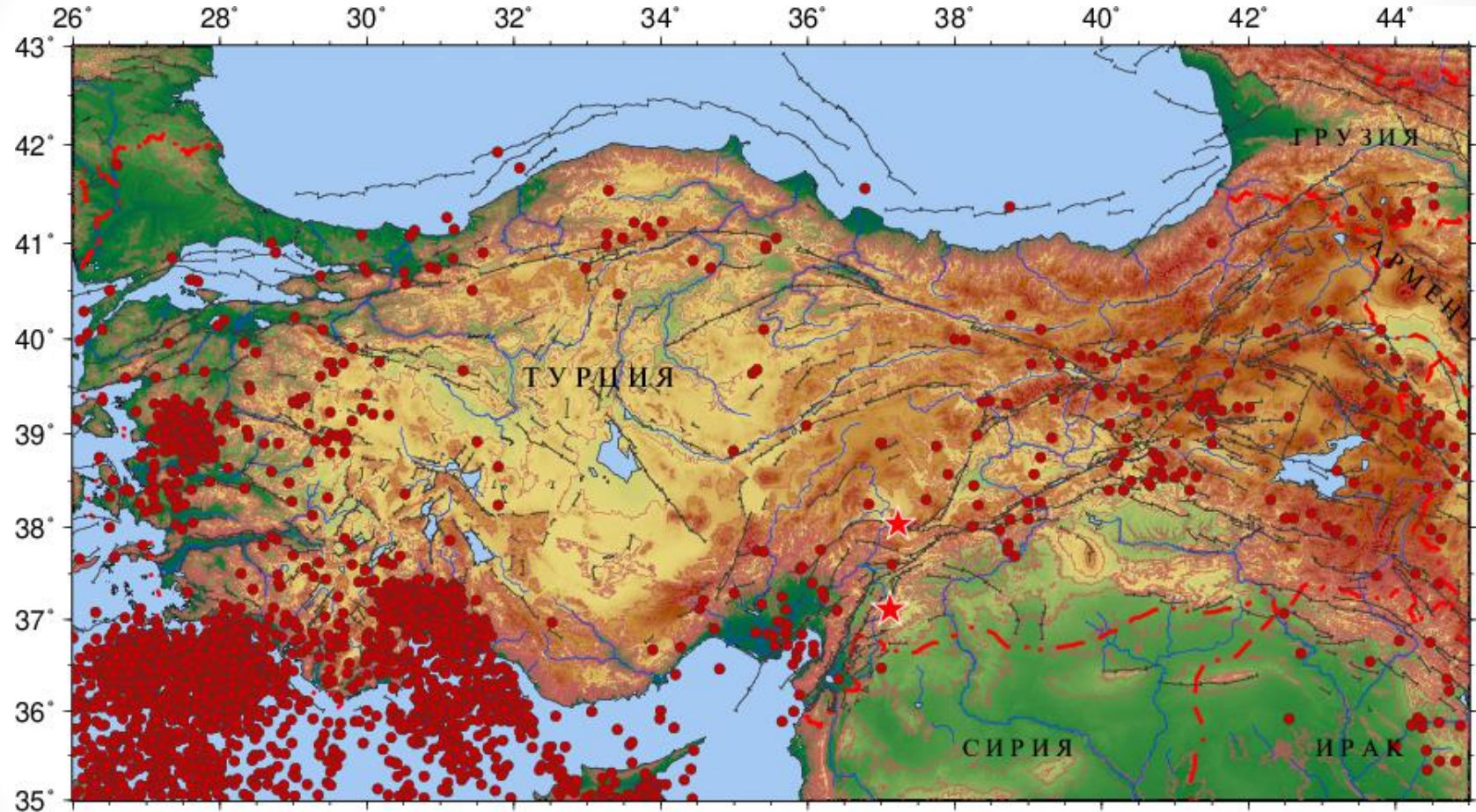


Fig. 9. Location of earthquakes with a depth of more than 50 km

Method

To assess the stress-strain state of the study area, the STD method is used, which is described in many works [Lukk, Yunga, 1979; Riznichenko, 1985; Jung, 1990; etc.] and remains relevant at the present time [Lukk et al., 2015; Sycheva, Mansurov, 2017; Lukk, Shevchenko, 2019; etc]. For a set of earthquakes that occurred in the volume of the medium V over a period of time T , the averaged inelastic deformation caused by them is described by the discontinuous (seismotectonic) deformation rate tensor $\langle \varepsilon_{ij} \rangle$ [Yunga, 1990; Riznichenko, 1985]:

$$\langle \varepsilon_{ij} \rangle = \frac{1}{\mu VT} \sum_{\alpha=1}^N M_0^{(\alpha)} m_{ij}^{(\alpha)} \quad (1)$$

where the summation is carried out over seismic events numbered using the index α , N is the number of events. In expression (1), $M_0^{(\alpha)}$ is the seismic moment of the earthquake with number (α) , $m_{ij}^{(\alpha)}$ is the direction tensor of the mechanism, μ is the shear modulus, V is the volume under study, and T is the study time. In the case when the time period is expressed in years, the $\langle \varepsilon_{ij} \rangle$ tensor is also called the average annual increase in seismotectonic deformation. In [Yunga, 1990; Lukk, Yunga, 1979] it is proposed to approximate (1) by the following expression:

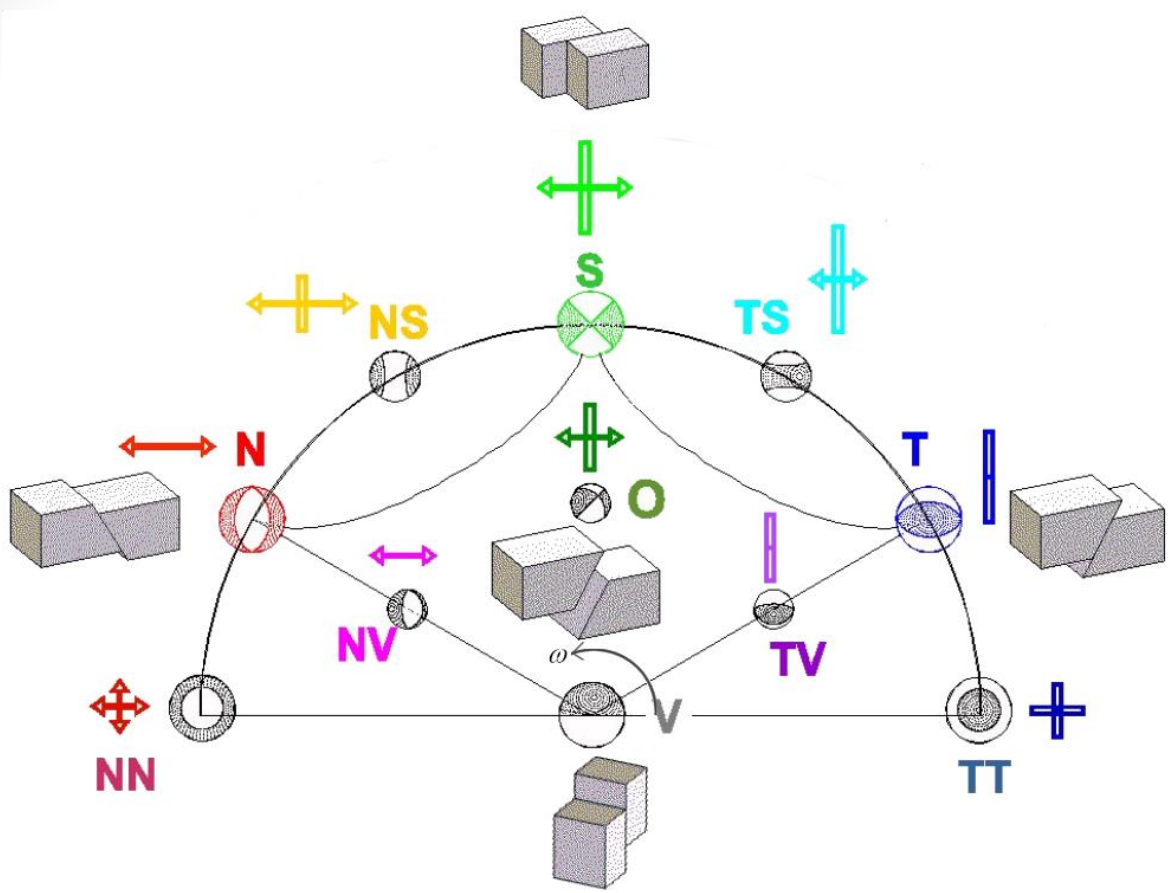
$$\langle \varepsilon_{ij} \rangle = \frac{1}{\mu VT} \sum_{\alpha=1}^N M_0^{(\alpha)} \cdot \sum_{\alpha=1}^N m_{ij}^{\alpha} = I_{\Sigma} \cdot \sum_{\alpha=1}^N w^{(\alpha)} m_{ij}^{\alpha} / \sum_{\alpha=1}^N w^{(\alpha)} \quad (2)$$

where $w(\alpha)$ is the weight of an individual event, determined from the weight function w [Yunga, 2002], and a scalar characteristic of the increase in seismotectonic deformation I_{Σ} , called the STD intensity, is introduced.

$$I_{\Sigma} = \frac{1}{\mu VT} \sum_{\alpha=1}^N M_0^{(\alpha)} \quad (3)$$

When calculating the direction of seismotectonic deformation by averaging the initial data, the geostructural region is subdivided into elementary subregions with a certain radius, the centers of which are located at the nodes (nodal points) of a specially selected grid. The STD calculation is performed by summing the matrices of individual mechanisms within each elementary subdomain. The STD intensity is calculated by summing the scalar seismic moments within each area according to [Lukk, Yunga, 1979]. For STD mapping, a classification of seismotectonic deformation regimes is used, based on parametrization through a system of angular parameters that provides an isometric mapping of tensor objects onto a sphere [Yunga, 1990, 1997].

Classification of STD modes



- Main modes:**
- T** – Thrust fault;
- N** – Normal fault;
- S** – Strike-slip ;
- V** – Vertical fault;
- Limit modes:**
- TT** – Thrust- Thrust fault;
- NN** – Normal –Normal fault;
- Transient modes:**
- TS** – Transpression;
- NS** – Transtension;
- TV** – Underpressional;
- NV** – Undertensional
- Detached mode:**
- O** – Oblique;

Fig. 10. Classification of STD modes according to [Junga, 1997].

Junga C.L. 1997. On the classification of tensors of seismic moments based on their isometric mapping to a sphere. *Dokl. RAS.* 352 (2): 253-255.

STD map

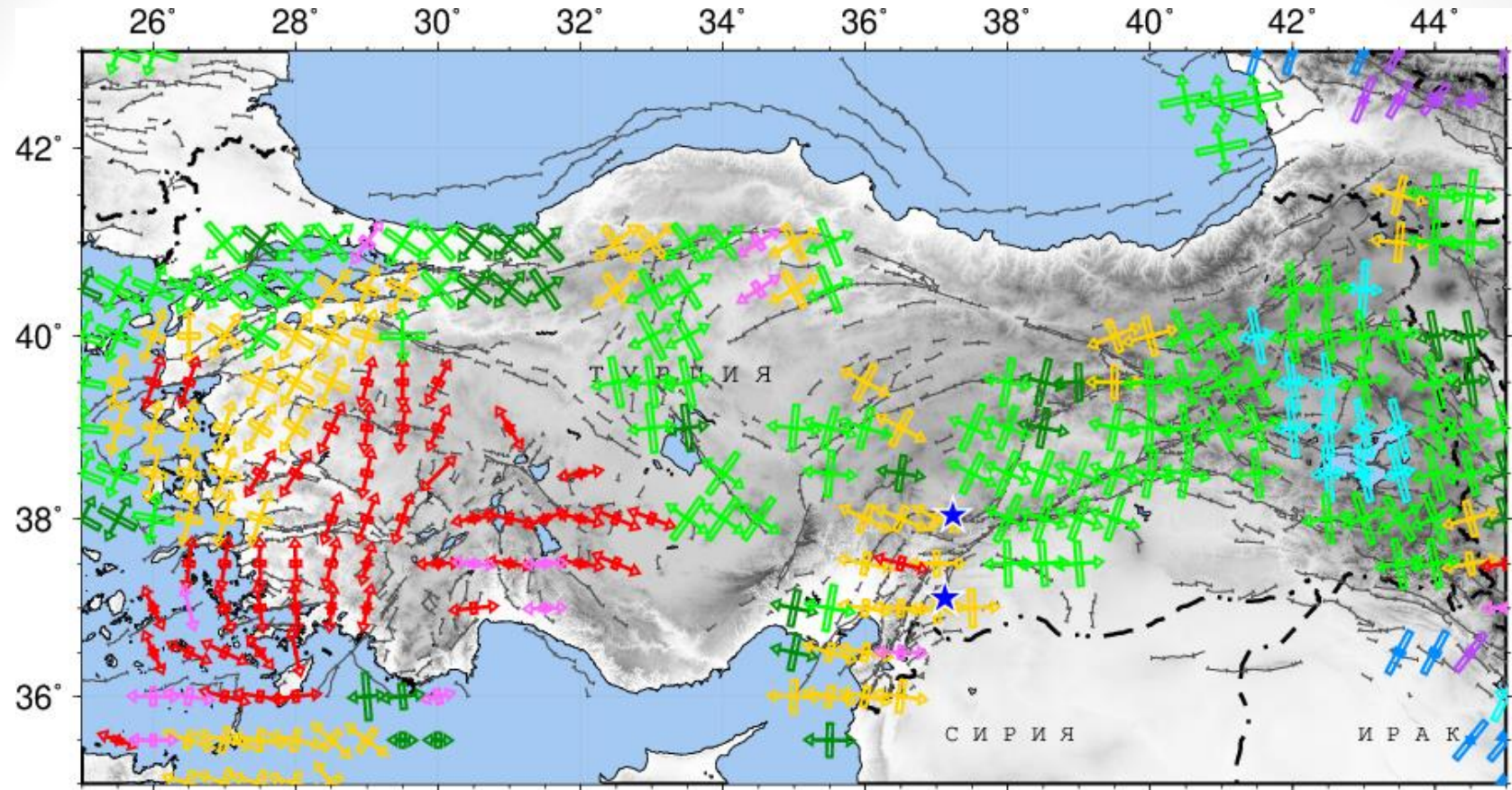
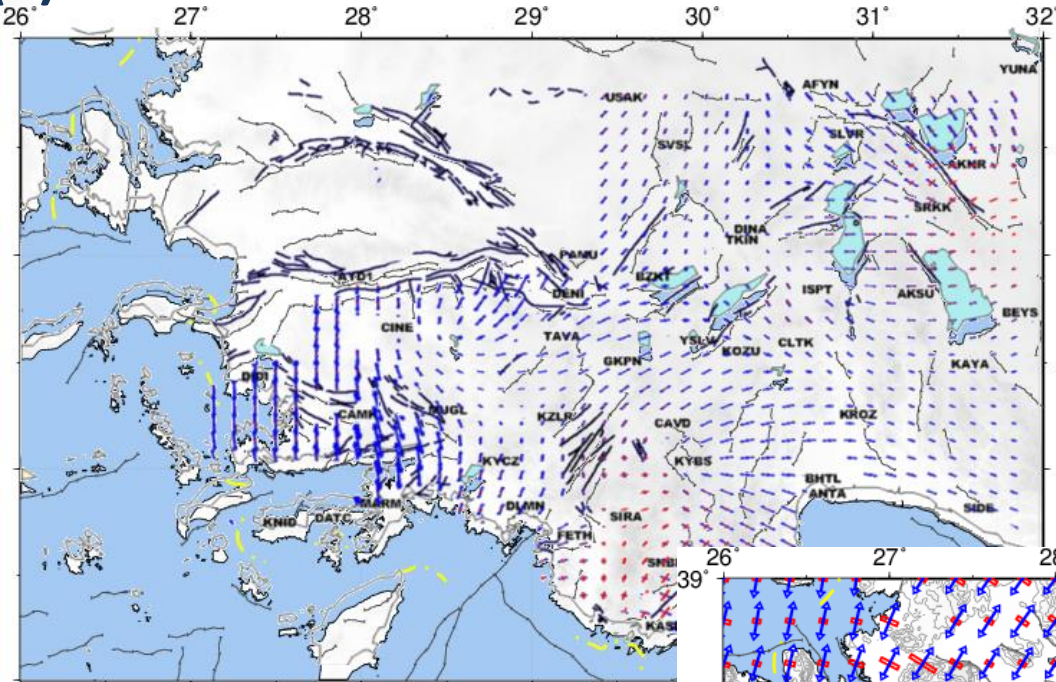


Fig. 11. STD map of Turkey.

Comparing STD and GPS data

(a)



Gülal E., Tiryakioglu I., Erdogan S., Aykut N.O., Baybura T., Akpınar B., A.K. Telli A.K., Ata E., Gümüş K., Taktak F., Yılmaz I., Öcalan T., Kalyoncuoglu Ü.Y., Dolmaz M.N., Elitok Ö, Erdogan H., Soyacan M., 2013. Tectonic activity inferred from velocity field of GNSS measurements in Southwest of Turkey. *Acta Geodaetica et Geophysica*. 109–121. DOI: 10.1007/s40328-012-0005-1.

(b)

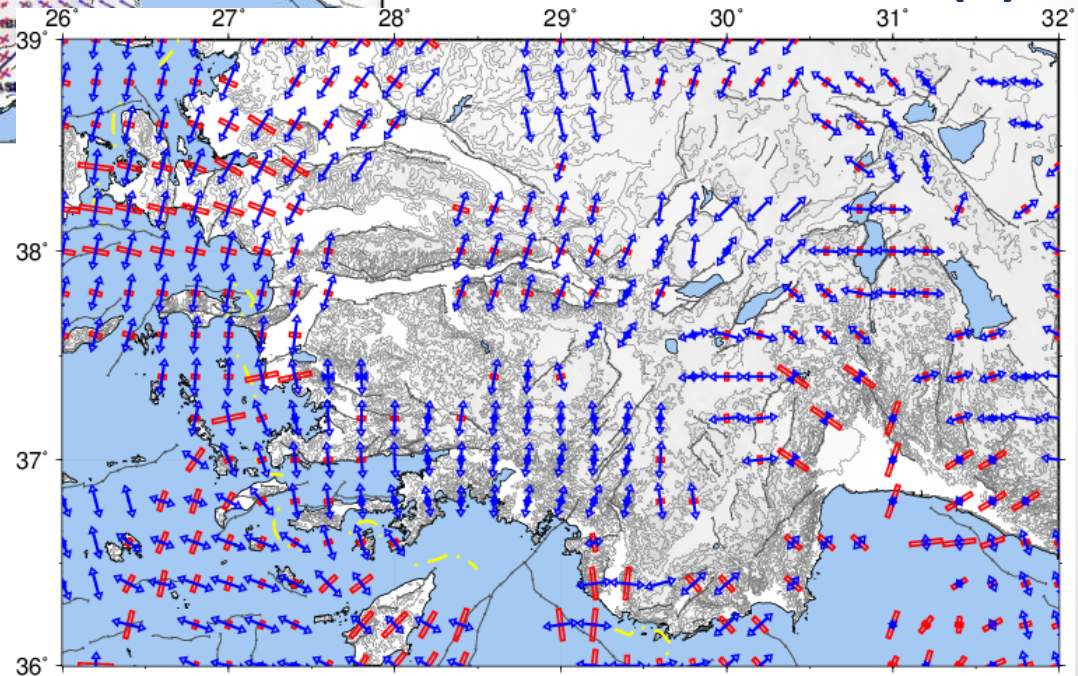


Fig. 12. Horizontal deformation velocity calculated from velocity vectors in the Fethiye-Burdur fault zone (FBRZ) [Gülal et al., 2013] and STD map .

Comparing STD and GPS data (Pamir)

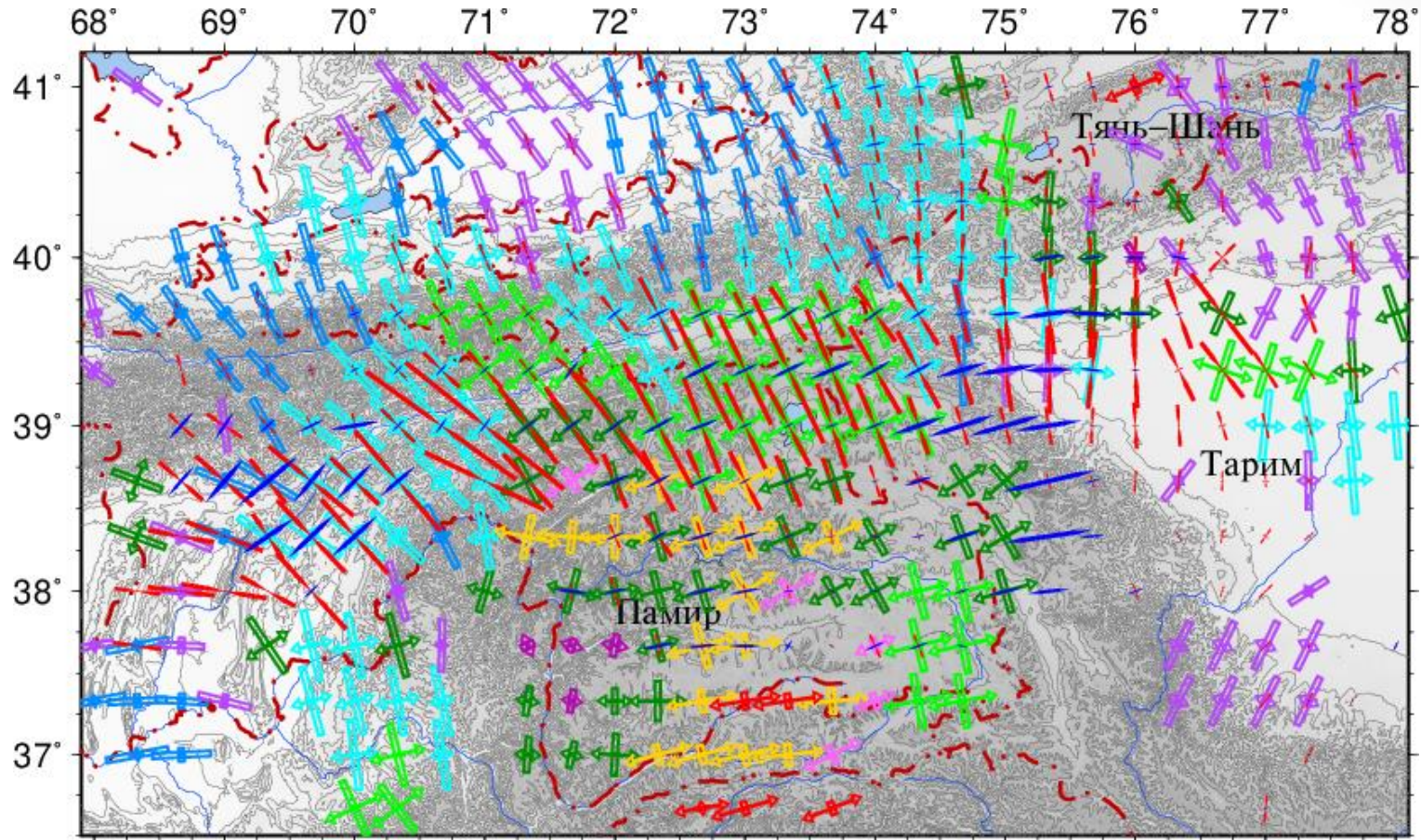


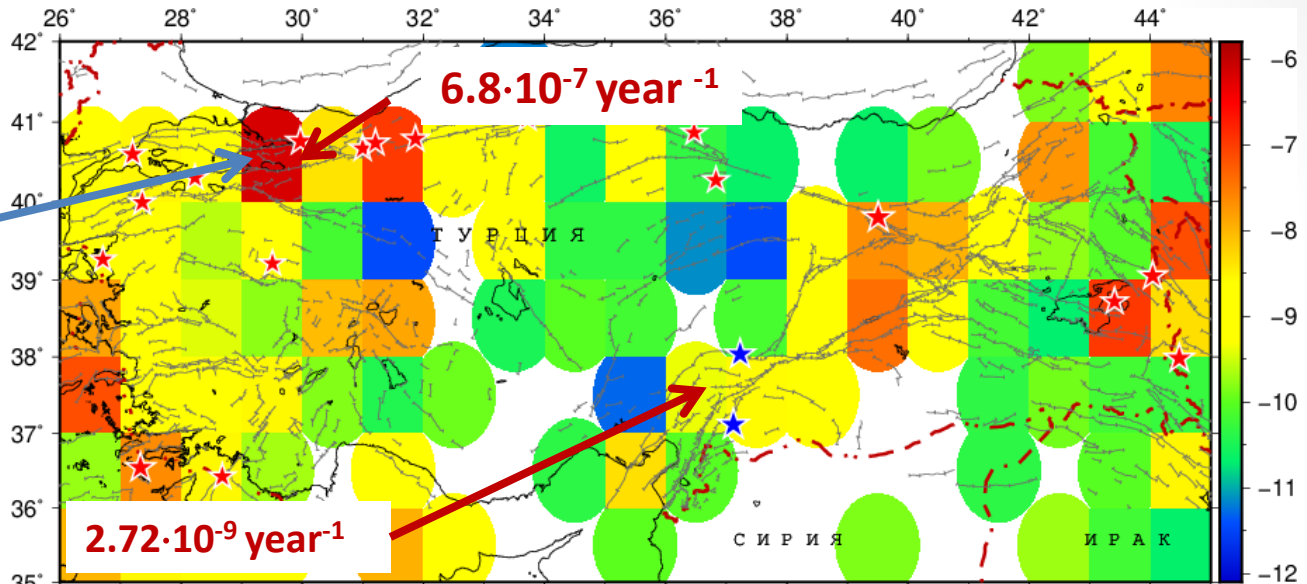
Fig. 13. Combined maps of STD directions and values of the strain rate tensor of the Earth's surface according to GNSS data (red is the shortening axis, blue is the elongation axis) for the Pamir and the immediate environment. The median difference is **8°**. The average difference is **12°**.

STD intensity

1976-2022

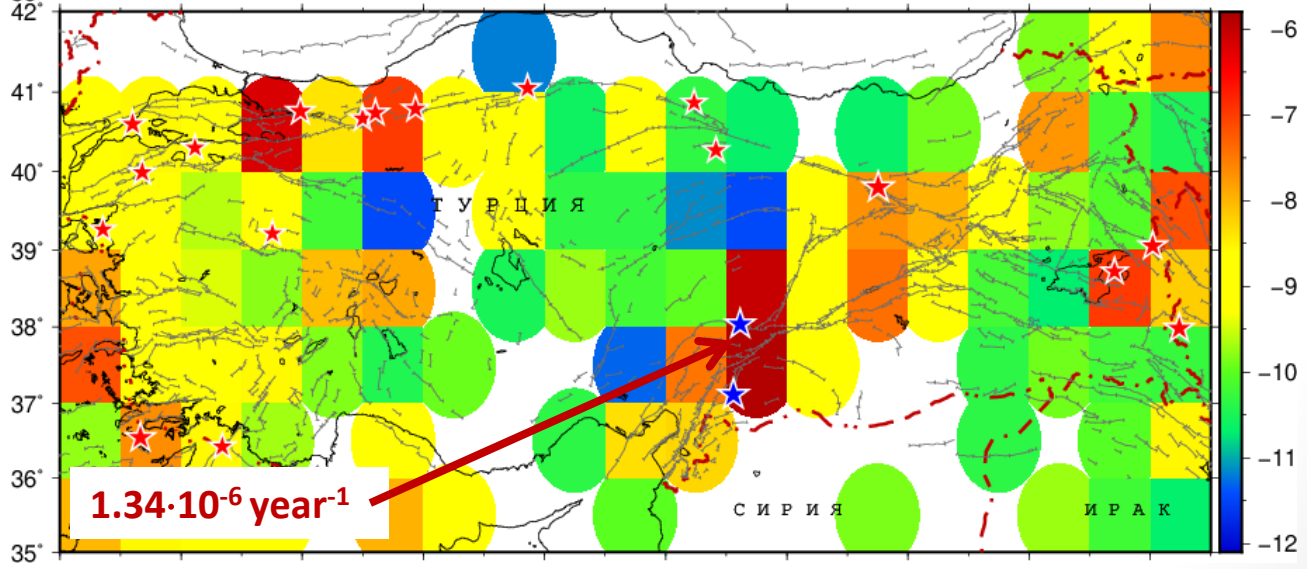
17.08.1999

M=7.6,
Kocaeli



a

1976-2023



b

Fig. 14. Distribution of the logarithm of the STD intensity (807 events, 1976 -2023) without taking into account data for 2023 (a) and taking into account 2023 (b).

Lode-Nadai, μ_ε

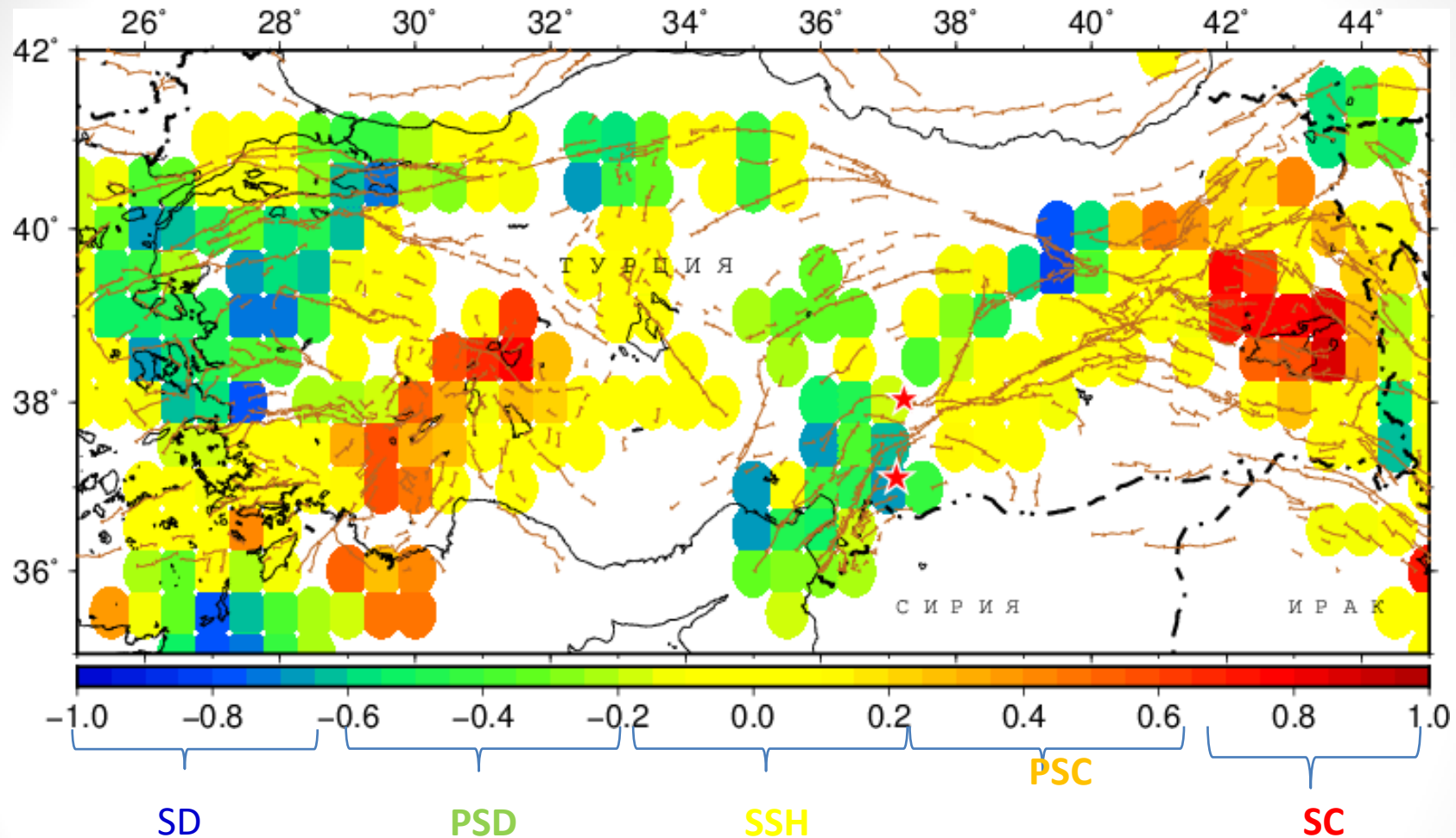


Fig. 15. Distribution of the Lode-Nadai coefficient.

Vertical component

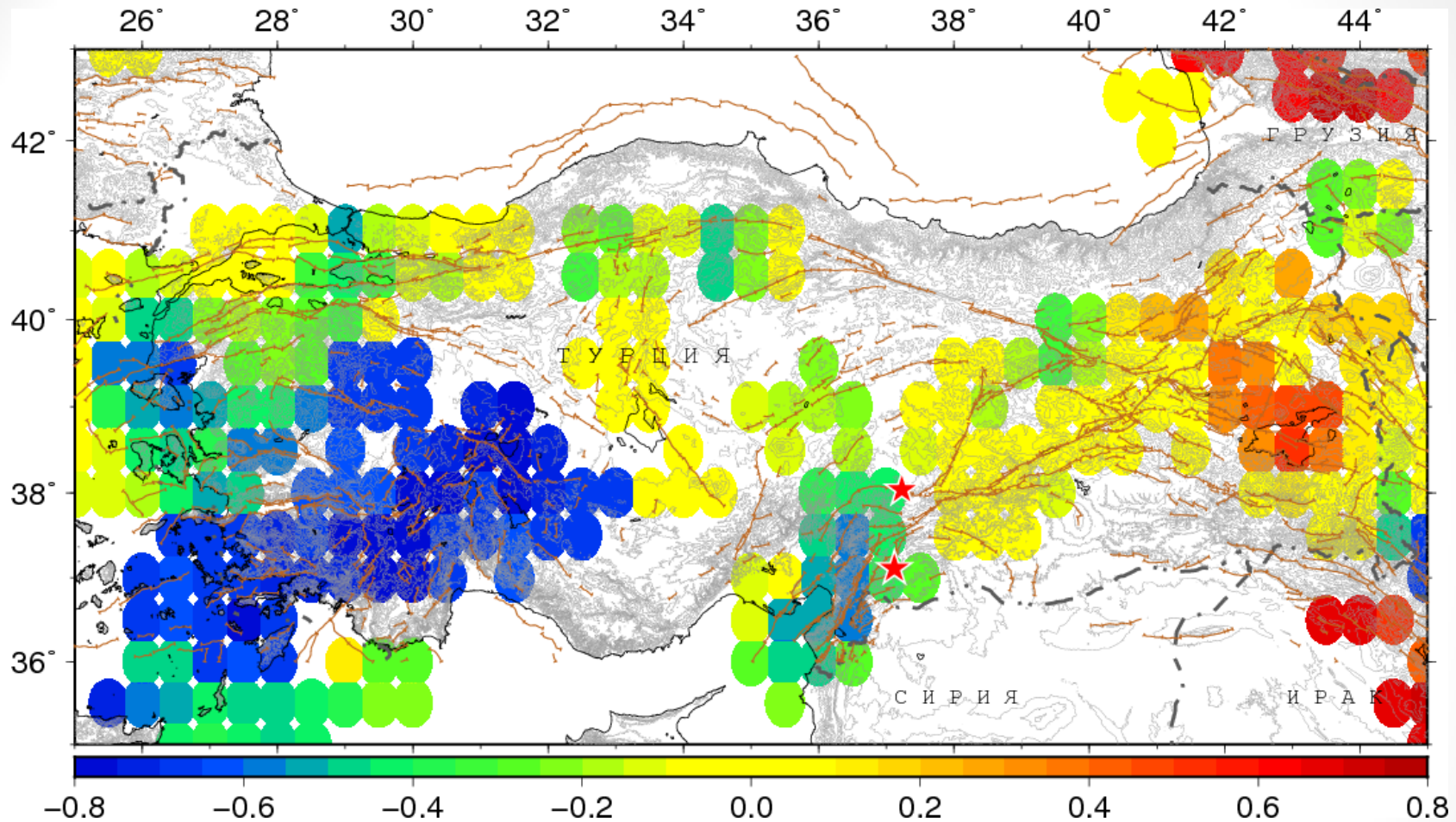


Fig. 16. Distribution of vertical component.

The value of the vertical component reflects the vertical movements of the earth's crust - negative values indicate its subsidence, positive values indicate uplift.

Conclusion

1. Based on the classification of STD modes, a map of STD was constructed. A variety of STD modes are observed in the study area: horizontal shear (eastern and central parts of Turkey), transtension (southern part of the EAF and coastal western part of Turkey), extension (southwestern part of Turkey), and transpression (Lake Van area).
2. Comparison of deformation models obtained for the Fethiye-Burdur Fault (FBFZ) from seismic and GNSS data showed good compatibility of the directions of the elongation and shortening axes.
3. According to the results of constructing the distribution of the Lode - Nadai coefficient, a significant part of the territory is characterized by a simple shear regime, the western part of Turkey experiences deformation with a predominance of simple tension, in the vicinity of Lake Van - a deformation with a predominance of simple compression.
4. The western part of Turkey, as well as the southern part of the East Anatoli fault system, is experiencing a subsidence of the territory, and the area of Lake Van is experiencing an uplift.



• Thank you for your attention

Akhtamar Island on Lake Van